DE GRUYTER High Temperature Materials and Processes 2023; 42: 20220255

Research Article

Shishi Wei, Xuan Xiao*, Kai Zhou, Jing Yao, and Dezhi Chen

First-principles investigation of phase stability and elastic properties of Laves phase $TaCr_2$ by ruthenium alloying

https://doi.org/10.1515/htmp-2022-0255
received September 26, 2022; accepted November 08, 2022

Abstract: Based on the first-principles method of density functional theory, the microscopic mechanism of the effect of addition of alloying element Ru content on the stability and elastic properties of Laves phase $TaCr_2$ was investigated by parameters such as formation enthalpy, electronic structure, and elastic constants. The addition of Ru atoms tends to preferentially occupy the lattice sites of Cr. With the increase in the Ru content, the alloying ability of $Ta_8Cr_{16-n}Ru_n$ (n = 0–6) becomes progressively weaker, the stability gradually decreases, whereas the Poisson's ratio grows. The bonding peak appears to drop and widen, weakening the bonding strength of Ta–Cr atoms, rendering the shear deformation to be performed easily, thereby improving toughness. When the Ru content rises to 20.83 at%, the bulk modulus, shear modulus, Young's modulus, and Poisson's ratio of the alloy attain the maximum value, the brittleness diminishes to the most extent, the resistance to elastic deformation is the strongest, as well at the optimum fracture toughness.

Keywords: ruthenium alloying, Laves phase $TaCr_2$, phase stability, elastic properties, first-principles

1 Introduction

Laves phase $TaCr_2$ alloy with high melting point (2,020°C), moderate density (10.7 g·cm^{-3}), a combination of good high-temperature strength, and creep resistance, is a new high temperature structural material with promising applications [1–8]. Nevertheless, the room temperature brittleness of Laves phase $TaCr_2$ alloys severely limits their practical applications [9,10]. Doping alloying elements is an essential strategy to improve the room temperature brittleness of Laves Phase alloys [11–19]. The first-principles calculations can reveal the microscopic mechanisms by which element types and varying atomic percentages of concentrations affect the mechanical properties of the alloys [20–30]. Huang et al. [31] investigated the impact of nickel alloying on the fracture toughness of $NbCr_2$ based on first-principles calculations method. It was found that Ni tended to occupy the Cr site, and the fracture toughness values of $NbCr_2$ alloys were significantly improved with the addition of Ni atomic percentage content of 4.17 at%, reaching 1.45, 1.51, and 1.74 MPa·m$^{1/2}$ in the direction of (100), (110), and (111) Miller indices, respectively. Nickel alloying significantly enhanced the fracture toughness of Laves phase $NbCr_2$. Liu et al. [32] studied the occupation mode, generalized stacking layer dislocation energy, and surface energy of the doped elements M (V, Zr, Mo) in $NbCr_2$ alloy and M (V, Ta, W) in $HfCr_2$ according to the first-principles calculation method. When Mo took up the Nb sites in $NbCr_2$ and Ta or W occupied Hf sites in $HfCr_2$, the toughness of $NbCr_2$ and $HfCr_2$ was improved. The doping of alloying elements can alter the electron concentration, elastic modulus, lattice constant, and stacking layer dislocation energy of Laves phase intermetallic compounds, and form vacancy defects and trigger lattice distortion, thus the bonding characteristics are modified and the resistance to dislocation movement is lessened, which will result in the improvement of plastic deformation capacity and in the enhancement of toughness of Laves phase intermetallic compounds.

The ideal atomic ratio R_A/R_B of AB_2 intermetallic compound is 1.225. If another ternary atom X is incorporated to

---

* **Corresponding author: Xuan Xiao,** School of Aeronautical Manufacturing Engineering, Nanchang Hangkong University, Nanchang 330063, China, e-mail: 70102@nchu.edu.cn
Shishi Wei, Kai Zhou: School of Aeronautical Manufacturing Engineering, Nanchang Hangkong University, Nanchang 330063, China
Jing Yao: School of Material Science and Engineering, Nanchang Hangkong University, Nanchang 330063, China
Dezhi Chen: School of Environmental and Chemical Engineering, Nanchang Hangkong University, Nanchang 330063, China

cause $R_A > R_x > R_B$, the ideal atomic ratio will be transformed and the free volume in the topologically dense crystal structure will be expanded, thus contributing to the occurrence of shear deformation and eventually toughening. The atomic radius of elements Ta, Cr, and Ru are 1.48, 1.27, and 1.32 Å, respectively, which meet the atomic size relationship $R_{\mathrm{Ta}} > R_{\mathrm{Ru}} > R_{\mathrm{Cr}}$. In accordance with the atomic size theory, it is concluded that the alloying of element Ru can enhance the toughness of $TaCr_2$. Tien et al. [11] investigated the effect of alloying element Ru on the mechanical properties of hot-pressed Ta–12.5Cr alloy and found that the addition of Ru increased the hardness; however, the addition of Ru did not effectively improve the fracture toughness, and further studies on the mechanical properties of Cr–Ta–Ru alloys with lower Ta content are desirable to clarify the effect of Ru in Cr-based two-phase alloys. Among the C36, C14, and C15 structures of Laves phase $TaCr_2$, the highest structural stability is C15–$TaCr_2$ [33]. Consequently, the effect of adding different contents of the element Ru on the phase stability and elastic properties of the C15-$TaCr_2$ will be illuminated in this study by means of first- principles calculation method.

2 Computational models and methods

2.1 Computational models

C15-$TaCr_2$ has a face-centered cubic structure with space group $Fd\bar{3}m$ (227) and cell parameters $a = b = c = 6.9850$ Å, $\alpha = \beta = \gamma = 90°$, with 24 atoms in the supercell, Ta atoms occupying the location of 8a (0, 0, 0) and Cr atoms occupying the position of 6d (0.625, 0.625 0.625). The doping element Ru is assigned to substitute the Ta or Cr atom in the cell of Ta_8Cr_{16} with an atomic concentration ratio of 4.17 at%, the molecular formulas are Ta_7RuCr_{16} and $Ta_8Cr_{15}Ru$, and the structural models are as presented in Figure 1(a) and (b), respectively. In order to achieve Ru alloying, Ta or Cr atoms with varying amounts of n are substituted in the supercell Ta_8Cr_{16}, the molecular formulas are $Ta_{8-n}Ru_nCr_{16}$ and $Ta_8Cr_{16-n}Ru_n$ (n = 0, 1, 2, 3, 4, 5, and 6), where the Ru content (at%) is 0, 4.17, 8.33, 12.50, 16.67, 20.83, and 25.00, respectively.

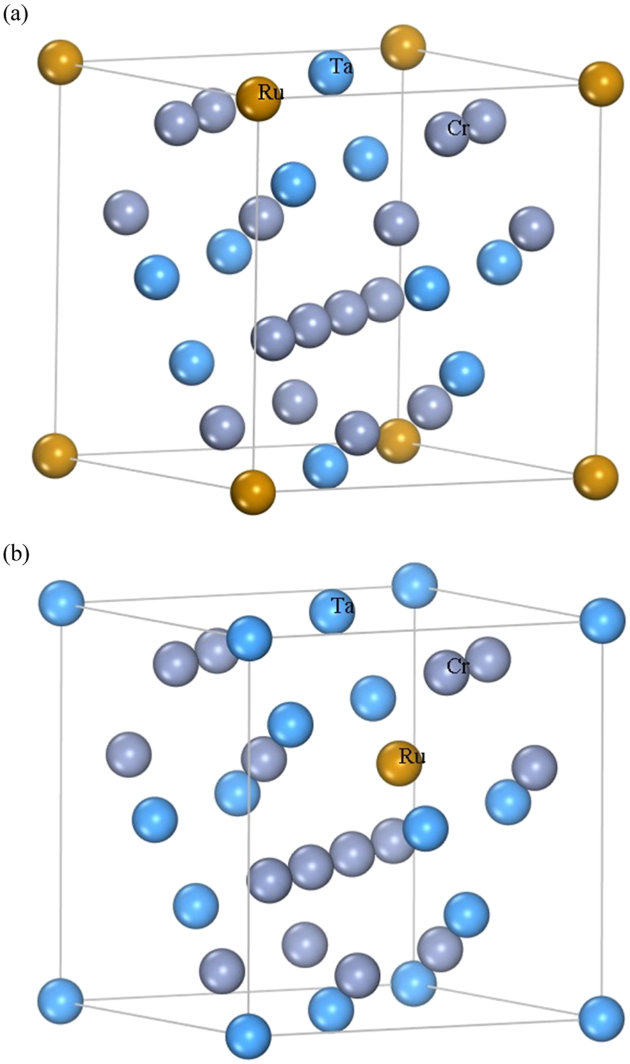

Figure 1: (a) Supercell model of Ta_7RuCr_{16} and (b) supercell model of $Ta_8Cr_{15}Ru$.

2.2 Computational methods

The Cambridge serial total energy package software based on density functional theory was used to calculate the potential function using an ultrasoft pseudopotential expressed in inverse space [34], and generalized gradient approximation in the Perdew–Burke–Ernzerhof method [35] to calculate the exchange correlation energy. The cutoff energy of the plane wave after convergence tests were taken as 450 eV, and the number of K-point grids by the Monkhorst-Pack method [36] was 4 × 4 × 4. The geometric structures were optimized through the Broyden–Fletcher–Goldfarb–Shannon algorithm [37], the total energy E of the self-consistent calculation system was 1.0×10^{-5} eV·atom^{-1}, the maximum force $F_{\max}$ on each atom was 0.03 eV·Å^{-1}, the stress deviation $S_{\max}$ was 0.05 GPa, and the tolerance shift $D_{\max}$ was 1.0×10^{-3} Å. The calculated $TaCr_2$ for the C15 structure lattice constant is $a = b = c =$ 6.9779 Å, which is in close match with the experimental values in the literature listed in Table 1.

3 Results and analysis of the calculation

3.1 Formation enthalpy and lattice constants

The lattice occupancy of the doped atoms in the C15-$TaCr_2$ is determined by the occupancy energy. In purpose of identifying the reasonable lattice occupancy of the doped Ru elements in $TaCr_2$ at Ta or Cr sites, the occupancy energy is figured out by the following equation:

$$E_{\mathrm{site}} = H_{\mathrm{A}} - H_{\mathrm{B}}, \tag{1}$$

where H_{A} and H_{B} are the formation enthalpies of Ta_7RuCr_{16} and $Ta_8Cr_{15}Ru$, respectively. When $E_{\mathrm{site}} > 0$, it refers to the tendency of Ru to occupy the lattice position of Cr atoms in the C15-$TaCr_2$ cell, and the larger the value of E_{site}, the stronger the tendency to preferentially take up the lattice site of Cr atoms. On the contrary, if the value of $E_{\mathrm{site}} < 0$, it indicates that Ru tends to occupy the lattice position of Ta atoms, and the smaller the value of E_{site}, the more obvious the tendency to preferentially occupy the lattice location of Ta atoms. The formulas for calculating the formation enthalpy H_{A} and H_{B} of Ta_7RuCr_{16} and $Ta_8Cr_{15}Ru$ are

$$H_{\mathrm{A}} = \frac{E_{\mathrm{total}}^{\mathrm{Ta_7RuCr_{16}}} - 7E_{\mathrm{solid}}^{\mathrm{Ta}} - E_{\mathrm{solid}}^{\mathrm{Ru}} - 16E_{\mathrm{solid}}^{\mathrm{Cr}}}{24}, \tag{2}$$

$$H_{\mathrm{B}} = \frac{E_{\mathrm{total}}^{\mathrm{Ta_8Cr_{15}Ru}} - 8E_{\mathrm{solid}}^{\mathrm{Ta}} - 15E_{\mathrm{solid}}^{\mathrm{Cr}} - E_{\mathrm{solid}}^{\mathrm{Ru}}}{24}, \tag{3}$$

where $E_{\mathrm{total}}^{\mathrm{Ta_7RuCr_{16}}}$ and $E_{\mathrm{total}}^{\mathrm{Ta_8Cr_{15}Ru}}$ are the total energy of Ta_7RuCr_{16} and $Ta_8Cr_{15}Ru$, $E_{\mathrm{solid}}^{\mathrm{Ta}}$, $E_{\mathrm{solid}}^{\mathrm{Cr}}$, and $E_{\mathrm{solid}}^{\mathrm{Ru}}$ represents the average energy of each Ta, Cr, and Ru atom in the ground state, respectively. Table 2 illustrates the ground state energies E_{solid} for individual atoms of Ta, Cr, and Ru. The enthalpies of formation H_{A} and H_{B} for Ta_7RuCr_{16} and $Ta_8Cr_{15}Ru$ are −3.3554 and −4.2424 eV, respectively, and the lattice occupation energy E_{site} is greater than 0. It can be concluded that Ru atoms tend to preferentially occupy the sites of Cr atoms. The calculated results are consistent with the experimental results [11].

Table 2: Ground state and freedom energy for Ta, Cr, and Ru atoms

Atom	E_{solid}(eV)
Ta	−137.1187
Cr	−2467.6458
Ru	−2602.2481

The geometrical optimization of the ternary phase after doping with Ru elements of different atomic percentage concentrations is conducted from the spatial position of the doped Ru elements occupying the C15-$TaCr_2$, and the formation enthalpy and lattice constant changes are calculated and analyzed. The formation enthalpy H_n of $Ta_8Cr_{16-n}Ru_n$ is formulated as

$$H_n = \frac{E_{\mathrm{total}}^{\mathrm{Ta_8Cr_{16-n}Ru_n}} - 8E_{\mathrm{solid}}^{\mathrm{Ta}} - (16 - n)E_{\mathrm{solid}}^{\mathrm{Cr}} - nE_{\mathrm{solid}}^{\mathrm{Ru}}}{24}. \tag{4}$$

The formation enthalpy H_n and the lattice constants of Laves phase $Ta_8Cr_{16-n}Ru_n$ doped with varying concentrations of Ru elements following geometric optimization are exhibited in Table 3. With the increase in the doping concentration from 4.17 at% to 16.67 at%, the absolute values of formation enthalpy H_{n} of $Ta_8Cr_{16-n}Ru_n$ ($n = 1 \rightarrow 4$) gradually decline, which reflects that the alloying ability of forming ternary alloy gradually weakens as the doping concentration of Ru increases. When the Ru concentration continues to improve to 20.83 at% ($n = 5$), the absolute value of the formation enthalpy enlarges slightly. With further addition of Ru concentration to 25 at% ($n = 6$), the absolute value of the enthalpy of generation is 4.0150 eV at the minimum. According to Table 3 and the above lattice occupation calculations, it appears that the lattice constant of C15-$TaCr_2$ is 6.9779 Å. The lattice constant of the ternary Laves phase formed by adding Ru exhibits a significant increase. As the Ru concentration goes from 0 to 25 at%, the lattice constant of the corresponding $Ta_8Cr_{16-n}Ru_n$ ternary phase

Table 1: Cell parameters for Ta atom and C15–$TaCr_2$ alloy

	Ta	C15–$TaCr_2$
Crystal structure	BCC	FCC
Space group	$Im\bar{3}m$(229)	$Fd\bar{3}m$(227)
Lattice parameters (experimental)	$a = b = c =$ 3.0600 Å [35]	$a = b = c =$ 6.9850 Å [38]
Lattice parameters (this study)	$a = b = c =$ 2.9165 Å	$a = b = c =$ 6.9779 Å

Table 3: Formation enthalpy H_n and lattice constants of $Ta_8Cr_{16-n}Ru_n$ by doping Ru with different atomic percent concentrations

Crystalline cell	H_n (eV)	Lattice constants (Å)
$Ta_8Cr_{15}Ru_1$	−4.2424	6.9945
$Ta_8Cr_{14}Ru_2$	−4.1807	7.0159
$Ta_8Cr_{13}Ru_3$	−4.1023	7.0299
$Ta_8Cr_{12}Ru_4$	−4.0415	7.0466
$Ta_8Cr_{11}Ru_5$	−4.0450	7.0745
$Ta_8Cr_{10}Ru_6$	−4.0150	7.1002

progressively rises to a maximum of 7.1002 Å. With the radius of Ru atoms larger than that of Cr atoms, the substitution of Ru elements for Cr atoms will contribute to an enlargement of the volume of the cell system. When relaxation is undertaken for specific positions occupied by more atoms in a volume-optimized supercell, it will push up the volume of the entire cell system even further.

3.2 Density of states (DOS)

To comprehend the effect of Ru alloying on the electronic structure of $TaCr_2$, the DOS before and after alloying are computed. The total DOS and the fractional wave DOS of $TaCr_2$ are demonstrated in Figure 2. It can be noticed that the total DOS of $TaCr_2$ is mainly contributed by d electron orbitals, and the percentage of s and p electron orbitals rarely contributes to DOS. The external valence electrons of Ta and Cr are $6s^2 5d^3 4f^{14}$ and $4s^1 3d^5$, respectively, so the total DOS of $TaCr_2$ is mainly contributed by 5d electrons of states of Ta and 3d electrons of states of Cr, indicating that the d electron orbitals have a significant impact on the Laves phase $TaCr_2$ alloying. Electrons near the Fermi energy level play a dominant role in the formation of chemical bonds, so only the electronic structure near the Fermi energy level is analyzed. The shape of the bond peaking near the Fermi energy level can reveal the strength of the electronic hybridization reactions and the bonding intensity of the chemical bonds [39].

The electronic DOS of $Ta_8Cr_{16-n}Ru_n(x = 1–6)$ crystals in the −5–4.5 eV energy level region is depicted in Figure 3, and the dashed lines in the figure are the Fermi energy levels. With the improvement in Ru atom concentration, the bonding peaks in the $Ta_8Cr_{16-n}Ru_n$ exhibit declining and broadening. Moreover, with the Ru content greater than or equal to 12.50 at%, new bonding peaks appear near the −5 to −3 eV energy level (as shown by the arrows in Figure 3), which indicates that Ru atoms have formed bonding interactions with Ta and Cr atoms in the cell, and the replacement solid solution of Ru weakens the bonding strength of the Ta–Cr bond in $TaCr_2$. When Ru is enlarged up to 25 at% (n = 6), the new bonding peaks tend to vanish.

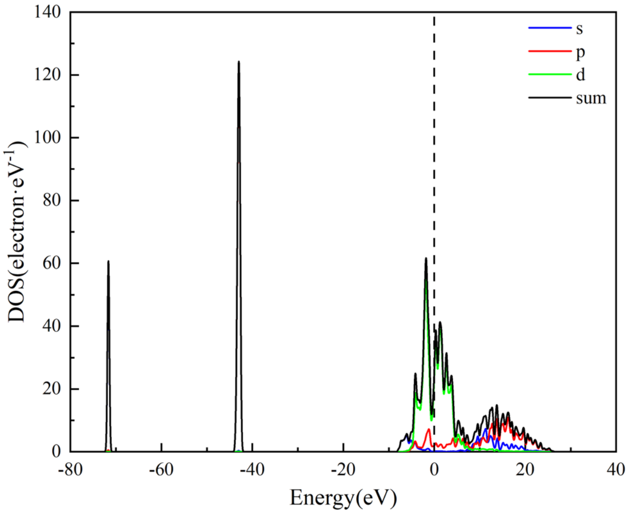

Figure 2: Total DOS and partial DOS of $TaCr_2$.

DOS of $TaCr_2$ alloys doped with various atomic percentage concentrations of Ru elements in the −3 to 2 eV energy level regions are illustrated in Figure 4. The energy of DOS of the initial Laves phase $TaCr_2$ and the Ru-doped alloy do not obviously change, and the bond peak DOS of $Ta_8Cr_{16-n}Ru_n$ ($n = 0 \rightarrow 6$) are measured to be 61.60, 56.53, 52.52, 49.05, 47.01, 44.43, and 42.76 electron·eV^{-1}. The significant reduction in the density of bonding peaks before and after doping indicates that the doping of Ru atoms weakens the hybridization reaction between the d electron orbitals of Ta and Cr, which in turn also leads to a reduction in the bonding strength of the chemical bond. It can also be viewed from Figure 4 that there are two more apparent spikes on both sides of the Fermi energy level, and the distance between the spikes is the pseudo-energy gap. In general, the wider the pseudo-energy gap, the stronger the bonding of the atoms of the alloy or compound and the more stable the structure. As the Ru doping concentration progressively proceeds from 4.17 to 25.00 at%, the pseudo-energy gap of $Ta_8Cr_{16-n}Ru_n$ ($n = 1 \rightarrow 6$) falls gradually from 2.10 eV to 1.85 eV, which implies that as the Ru content increases, the pseudo-energy gap increasingly becomes narrower and the alloy turns more unstable.

3.3 Elastic properties

The elastic constants are essential for a comprehension of the structural stability and bonding properties between adjacent atoms. Crystals of distinct crystal systems have different numbers of independent elastic constants. The C15 structure of Laves phase $TaCr_2$ has cubic symmetry and only three independent elastic constants, C_{11}, C_{12}, and C_{44}. The mechanical stability of cubic crystals has to be met [40]: $C_{11} - C_{12} > 0$, $C_{11} > 0$, $C_{44} > 0$, $C_{11} + 2C_{12} > 0$. The elastic constants of C15-$TaCr_2$ and $Ta_8Cr_{15}Ru$ are described as shown in Table 4. It is obvious that the

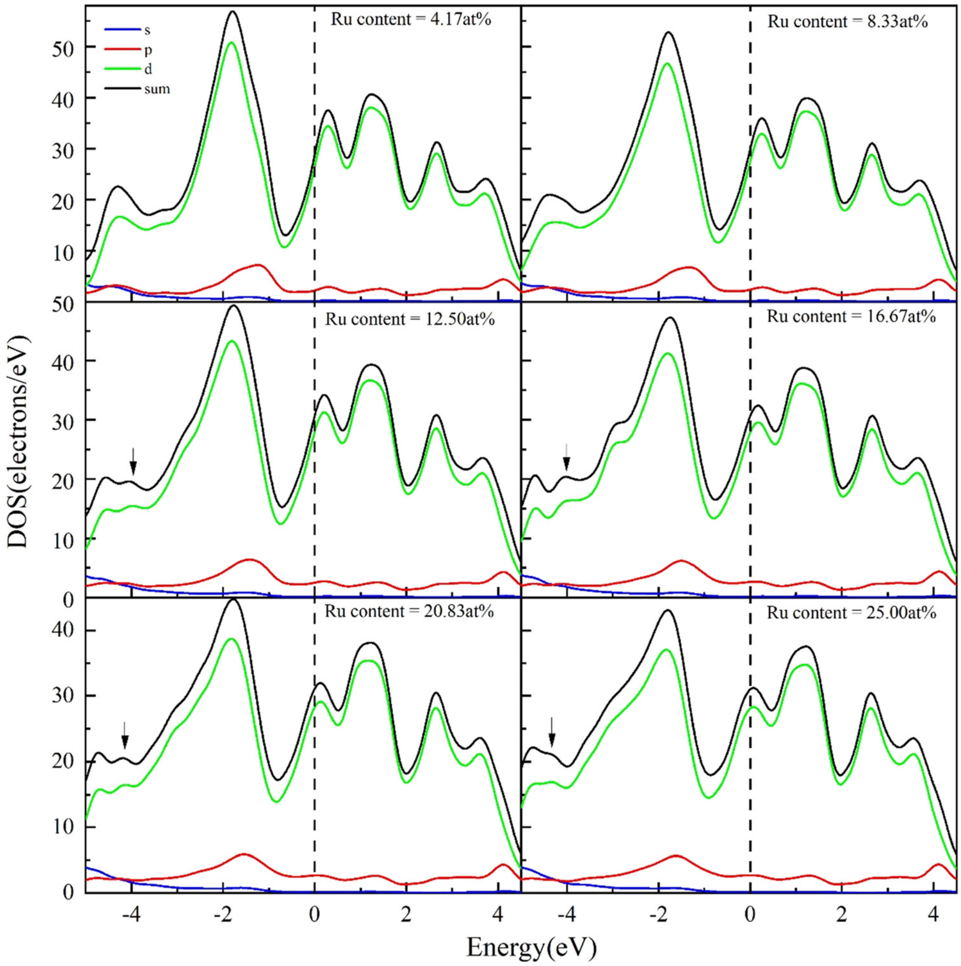

Figure 3: DOS of $Ta_8Cr_{16-n}Ru_n$(x = 1–6) alloys.

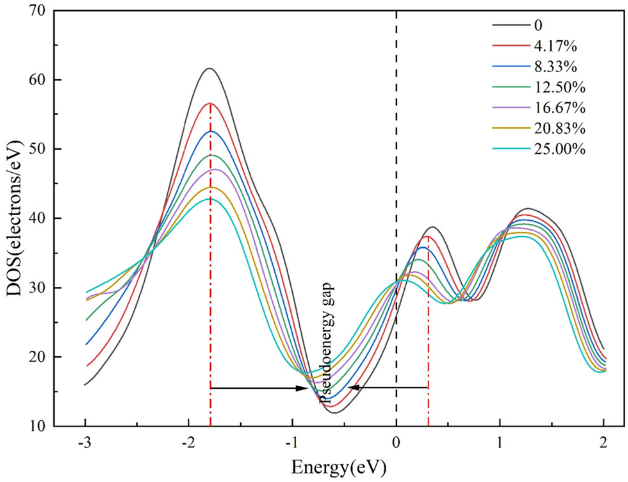

Figure 4: Total DOS of TaCr$_2$ alloys doped with different atomic percentages of Ru element in the energy level range of −3 to 2 eV.

elastic constants of $Ta_8Cr_{15}Ru$ and C15-TaCr$_2$ satisfy all the above inequalities, which suggests that they are stable in the ground state. The bulk modulus B, shear modulus G, Young's modulus E, Poisson's ratio v, and anisotropy constant A of the cubic structure can be directly calculated from the elastic constants, where the shear modulus G is the value of Hill model and the value of Hill model is the arithmetic average of Voigt model value G_V and Reuss value G_R [41], that is Voigt-Reuss-Hill approximation. The computational equation is as follows:

$$B = \frac{1}{3}(C_{11} + 2C_{12}), \tag{5}$$

$$G_V = \frac{1}{5}(C_{11} - C_{12} + 3C_{44}), \tag{6}$$

$$G_R = \frac{5C_{44}(C_{11} - C_{12})}{4C_{44} + 3(C_{11} - C_{12})}, \tag{7}$$

$$G = \frac{1}{2}(G_V + G_R), \tag{8}$$

$$E = \frac{9GB}{G + 3B}, \tag{9}$$

Table 4: Elastic constants for C15-$TaCr_2$ and $Ta_8Cr_{15}Ru$

Crystals	C_{11} (GPa)	C_{12} (GPa)	C_{44} (GPa)	*B* (GPa)	*G* (GPa)	*E* (GPa)	*V*	*B/G*	*A*
C15-$TaCr_2$	341	192	89	241	83	223	0.34	2.90	1.19
$Ta_8Cr_{15}Ru$	332	202	90	245	79	214	0.35	3.10	1.38
$TaCr_2$ Theo. [33]	347	218	88	261	78.6	214	0.363	3.32	1.36
$TaCr_2$ Theo. [44]	360	220	94	267	83	226	0.359	3.22	1.35
$TaCr_2$ Expt. [44]	281	173	73	209	64	175	0.360	3.26	1.34

$$v = \frac{3B - 2G}{6B + 2G}, \tag{10}$$

$$A = \frac{2C_{44}}{C_{11} - C_{12}}. \tag{11}$$

The bulk modulus *B* reflects the ability of the material to resist strain and the difficulty of deformation. The greater the value of *B*, the more difficult the material is for compression and deformation. After doping with alloying element Ru, the modulus of elasticity *B* increases from 241 to 245 GPa, and $Ta_8Cr_{15}Ru$ is more resistant to compression and deformation. The shear modulus *G* reflects the material's ability to resist shear strain, and the shear modulus *G* value of $Ta_8Cr_{15}Ru$ is lower than that of C15-$TaCr_2$, and the ability to resist shear strain of $Ta_8Cr_{15}Ru$ is lessened. Young's modulus *E* is commonly applied to embody the material's ability to resist elastic deformation. In a certain stress, the larger the *E* value, the smaller the elastic deformation, compared with the undoped system, the doping of Ru makes the Young's modulus *E* value of $TaCr_2$ decrease by 9 GPa, indicating that Ru doping makes the elastic deformation occur to a greater extent. The higher the value of Poisson's ratio *v*, the better the plasticity of the material, and the value is between –1 and 0.5. The results demonstrate that the plasticity of $Ta_8Cr_{15}Ru$ is better than that of C15-$TaCr_2$. The anisotropy constant *A* is adopted to quantify the degree of anisotropy of a solid. When *A* is equal to 1, the material is elastically isotropic, otherwise it is elastically anisotropic. The more the deviation of the *A* value from 1, the more pronounced the elastic anisotropy is. The *A* value of $Ta_8Cr_{15}Ru$ is more than that of C15-$TaCr_2$, which represents that the elastic anisotropy of the Ru-doped system is more obvious.

In accordance with the Pugh criterion [42], when the *B/G* ratio > 1.75, the alloy is ductile in character, otherwise it shows brittleness. All theoretical and experimental results were found to be greater than 1.75 on the basis of the *B/G* ratio in Table 4, illustrating that the Laves phase $TaCr_2$ has favorable plasticity. However, a multitude of experimental results reveal that $TaCr_2$ is a brittle intermetallic compound at room temperature with a minor fracture toughness value of about 1.0 MPa·$m^{1/2}$. The *B/G* criterion of Pugh was proposed based on pure metals rather than compounds, and the mechanical properties of the C15-$NbCr_2$ Laves phase and other Laves phases and some compounds exceed the *B/G* criterion of Pugh [43], and the brittleness and ductility of the compounds are more sophisticated, which rely on several factors such as crystal structure, electronic structure, chemical bonding, and deformation mechanisms.

The elastic constants of the ternary phase $Ta_8Cr_{16-n}Ru_n$ with varying percentage concentrations of Ru-doped elements are shown in Figure 5. The bulk modulus *B* changes slightly between 0 and 16.67 at% of Ru content, and the

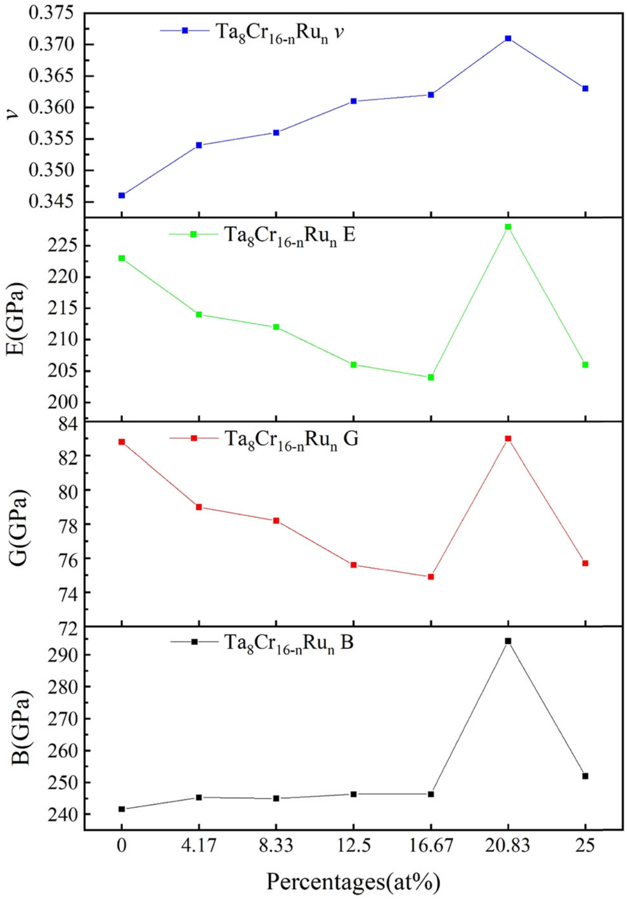

Figure 5: Elastic constants of ternary phases with different percentage concentrations of ruthenium alloying.

shear modulus G and Young's modulus E tend to decrease, and at the time of Ru content of 16.67 at%, the values of B, G, and E are all minimal, and meanwhile the hardness of $Ta_8Cr_{16-n}Ru_n$ is the smallest and the degree of elastic deformation is the largest. The Poisson's ratio v tends to rise with the increase in Ru concentration, and v reaches the maximum value of 0.371 at the Ru content of 20.83 at%, the brittleness reduces to a greater extent, and the B, G, and E values are obviously increasing, and the elastic deformation resistance is enhanced at this occasion. From the DOS in Figure 3, it can be noticed that with Ru content of 25 at%, the new bonding peak disappears and the difficulty of breaking the Ta–Cr chemical bond is enhanced relative to that with Ru content of 20.83 at% ($n = 5$), and the Poisson's ratio v declines slightly compared to the previous one at a Ru atomic percentage concentration of 20.83 at%, the improvement in brittleness is satisfactory and the enhancement of hardness is greater.

4 Conclusion

The lattice occupation energy calculations of Ta–Ru–Cr ternary alloys illustrate that Ru atoms tend to preferentially occupy the lattice positions of Cr atoms in C15-$TaCr_2$, and their alloying ability decreases with the increase in the Ru element content, while the absolute value of the generation enthalpy rises slightly when the Ru concentration is 20.83 at%. The atomic radius of Ru is larger than that of Cr, accounting for the continuous growth of the lattice constant of the alloy as Ru content rises. Ru alloying reduces the stability of $TaCr_2$, the pseudo-energy gap narrows and the stability decreases gradually. The elastic constants indicate that Ru alloying can reduce the brittleness of $TaCr_2$, and the bonding peaks are both decreased and broadened, which weakens the bonding strength of Ta–Cr atoms and improves the deformability of the material. When the Ru content is 16.67 at%, $Ta_8Cr_{16-n}Ru_n$ has the smallest hardness and the largest elastic deformation degree, and when the Ru concentration is 20.83 at%, the brittleness improvement effect is more obvious and the hardness is larger.

Acknowledgements: The authors gratefully acknowledge the fundamental support from the National Natural Science Foundation of China (Grant no. 52161021 and 51964034), the S&T plan projects of Jiangxi Provincial Department of Education (DA202101175), and Graduate Innovative Special Fund Projects of Jiangxi Province (YC2021-S676).

Funding information: National Natural Science Foundation of China (Grant no. 52161021 and 51964034), the S&T plan projects of Jiangxi Provincial Department of Education (DA202101175), and Graduate Innovative Special Fund Projects of Jiangxi Province (YC2021-S676).

Author contributions: Shishi Wei: data calculation and analyses, and wrote the manuscript; Xuan Xiao: methodology and supervision; Kai Zhou: conception of the study and manuscript preparation; Jing Yao: analysis; Dezhi Chen: manuscript preparation.

Conflict of interest: Authors state no conflict of interest.

References

[1] Guénolé, J., F. Z. Mouhib, L. Huber, B. Grabowski, and S. Korte-Kerzel. Basal slip in Laves phases: the synchroshear dislocation. *Scripta Materialia*, Vol. 166, 2019, pp. 134–138.

[2] Sun, F., J. Zhang, S. Mao, and X. Han. First-principles studies of the structural and electronic properties of the C14 Laves phase XCr_2 (X = Ti, Zr, Nb, Hf and Ta). *Philosophical Magazine*, Vol. 9319, 2013, pp. 2563–2575.

[3] Xian, Y., H. Zheng, Q. Zhai, and Z. Luo. A two-dimensional structure map for prediction of the transition-metal Laves phases. *Computational Materials Science*, Vol. 125, 2016, pp. 1–7.

[4] Wilson, A. S., E. J. Pickering, C. N. Jones, C. M. F. Rae, and H. J. Stone. Addition of Ge to Cr-Ta-Si laves phase-based alloys. *Intermetallics*, Vol. 138, 2021, id. 107311.

[5] Zubair, M., S. Sandlöbes, M. A. Wollenweber, C. F. Kusche, W. Hildebrandt, C. Broeckmann, et al. On the role of Laves phases on the mechanical properties of Mg-Al-Ca alloys. *Materials Science and Engineering: A*, Vol. 756, 2019, pp. 272–283.

[6] Rabadia, C. D., Y. J. Liu, L. Y. Chen, S. F. Jawed, L. Q. Wang, H. Sun, et al. Deformation and strength characteristics of Laves phases in titanium alloys. *Materials & Design*, Vol. 179, 2019, id. 107891.

[7] Xue, Y., N. Takata, H. Li, M. Kobashi, and L. Yuan. Critical resolved shear stress of activated slips measured by micropillar compression tests for single-crystals of Cr-based Laves phases. *Materials Science and Engineering: A*, Vol. 806, 2021, id. 140861.

[8] Yan, X., X. Q. Chen, A. Grytsiv, P. Rogl, R. Podloucky, V. Pomjakushin, et al. Crystal structure, phase stability and elastic properties of the Laves phase $ZrTiCu_2$. *Intermetallics*, Vol. 16, No. 5, 2008, pp. 651–657.

[9] Vedmedenko, O., F. Rösch, and C. Elsässer. First-principles density functional theory study of phase transformations in $NbCr_2$ and $TaCr_2$. *Acta materialia*, Vol. 5618, 2008, pp. 4984–4992.

[10] Bhowmik, A., C. N. Jones, I. M. Edmonds, and H. J. Stone. Effect of Mo, Al and Si on the microstructure and mechanical properties of Cr-Cr_2Ta based alloys. *Journal of Alloys and Compounds*, Vol. 530, 2012, pp. 169–177.

[11] Tien, R. H., J. H. Zhu, C. T. Liu, and L. R. Walker. Effect of Ru additions on microstructure and mechanical properties of

Cr-$TaCr_2$ alloys. *Intermetallics*, Vol. 13, No. 3–4, 2005, pp. 361–366.

[12] Bhowmik, A., S. Neumeier, J. S. Barnard, C. H. Zenk, M. Göken, C. M. Rae, et al. Microstructure and mechanical properties of Cr-Ta-Si Laves phase-based alloys at elevated temperatures. *Philosophical Magazine*, Vol. 9434, 2014, pp. 3914–3944.

[13] Brady, M. P., C. T. Liu, J. H. Zhu, P. F. Tortorelli, and L. R. Walker. Effects of Fe additions on the mechanical properties and oxidation behavior of Cr_2Ta Laves phase reinforced Cr. *Scripta Materialia*, Vol. 52, No. 9, 2005, pp. 815–819.

[14] Fujita, M., Y. Kaneno, and T. Takasugi. Phase field and room-temperature mechanical properties of C15 Laves phase in Nb-Hf-Cr and Nb-Ta-Cr alloy systems. *Journal of alloys and compounds*, Vol. 424, No. 1–2, 2006, pp. 283–288.

[15] Xue, Y., S. Li, Y. Wu, C. Liu, H. Liu, and L. Yuan. Strengthening and toughening effects in Laves phase Cr_2Ta/Cr *in situ* composites by Si additions. *Vacuum*, Vol. 174, 2020, id. 109202.

[16] Yao, Q., J. Sun, Y. Zhang, and B. Jiang. First-principles studies of ternary site occupancy in the C15 $NbCr_2$ Laves phase. *Acta materialia*, Vol. 5413, 2006, pp. 3585–3591.

[17] Ran, J. Q., M. W. Fu, and W. L. Chan. The influence of size effect on the ductile fracture in micro-scaled plastic deformation. *International Journal of Plasticity*, Vol. 41, 2013, pp. 65–81.

[18] Lu, S., H. Zheng, L. Deng, and J. Yao. Effect of silicon on the fracture toughness and oxidation behavior of hot pressed $NbCr_2$ alloys. *Materials & Design*, Vol. 51, 2013, pp. 432–437.

[19] Takasugi, T., M. Yoshida, and S. Hanada. Deformability improvement in C15 $NbCr_2$ intermetallics by addition of ternary elements. *Acta materialia*, Vol. 44, No. 2, 1996, pp. 669–674.

[20] Peng, L., S. Takizawa, K. I. Ikeda, T. Horiuchi, and S. Miura. Effect of Si on the stability of $NbCr_2$ Laves phase in Cr-Mo-Nb system. *Intermetallics*, Vol. 110, 2019, id. 106457.

[21] Tang, H., W. Xing, X. Li, B. Chen, P. Zhao, L. Shu, et al. Insights into the gradient-characteristic precipitation behaviors of Laves phase induced by Fe/W/Mo addition in $Ti_{42}Al_5Mn$ alloy. *Intermetallics*, Vol. 128, 2021, id. 107022.

[22] Chen, S., Y. Sun, Y. H. Duan, B. Huang, and M. J. Peng. Phase stability, structural and elastic properties of C15-type Laves transition-metal compounds MCo_2 from first-principles calculations. *Journal of Alloys and Compounds*, Vol. 630, 2015, pp. 202–208.

[23] Nong, Z. S., J. C. Zhu, Y. Cao, X. W. Yang, Z. H. Lai, and Y. Liu. A first-principles study on the structural, elastic and electronic properties of the C14 Laves phase compounds TiX_2 (X = Cr, Mn, Fe). *Physica B: Condensed Matter*, Vol. 419, 2013, pp. 11–18.

[24] Rabahi, L., B. Alili, D. Bradai, T. Grosdidier, and A. Kellou. DFT calculations of structural, magnetic and thermal properties of C15, C14 and C36 Laves phases in Fe-Nb-Zr. *Intermetallics*, Vol. 83, 2017, pp. 92–100.

[25] Du, J., A. Zhang, Z. Guo, M. Yang, M. Li, and S. Xiong. Atomic cluster structures, phase stability and physicochemical properties of binary Mg-X (X = Ag, Al, Ba, Ca, Gd, Sn, Y and Zn) alloys from ab-initio calculations. *Intermetallics*, Vol. 95, 2018, pp. 119–129.

[26] Kazantzis, A. V., M. Aindow, I. P. Jones, G. K. Triantafyllidis, and J. T. M. De. Hosson. The mechanical properties and the deformation microstructures of the C15 Laves phase Cr_2Nb at high temperatures. *Acta Materialia*, Vol. 55, No. 6, 2007, pp. 1873–1884.

[27] Li, C., K. Zhang, and J. G. Ru. Pressure dependence of structural, elastic and electronic of Mg_2Y: A first principles study. *Journal of Alloys and Compounds*, Vol. 647, 2015, pp. 573–577.

[28] Pluengphon, P., T. Bovornratanaraks, and U. Pinsook. Structural, electronic, optical and mechanical properties of InP alloyed with Zn, Si, Sn and S under pressure: First-principles calculation. *Journal of Alloys and Compounds*, Vol. 700, 2017, pp. 98–105.

[29] Hu, Y. L., L. H. Bai, Y. G. Tong, D. Y. Deng, X. B. Liang, J. Zhang, et al. First-principle calculation investigation of NbMoTaW based refractory high entropy alloys. *Journal of Alloys and Compounds*, Vol. 827, 2020, id. 153963.

[30] Li, C., J. Kuo, B. Wang, and R. Wang. Effects of X (V, W, Mo, Hf, Ta, Zr) additions on the ideal cleavage fracture of Cr_2Nb: First-principles determination. *Intermetallics*, Vol. 18, No. 1, 2010, pp. 65–69.

[31] Huang, H., G. Li, X. Xiao, S. Lu, and P. Peng. Micromechanism in fracture toughness of $NbCr_2$ Laves phase improved by nickel alloying: first-principles calculation. *Journal of Alloys and Compounds*, Vol. 857, 2021, id. 158040.

[32] Liu, L., P. Shen, X. Wu, R. Wang, W. Li, and Q. Liu. First-principles calculations on the stacking fault energy, surface energy and dislocation properties of $NbCr_2$ and $HfCr_2$. *Computational Materials Science*, Vol. 140, 2017, pp. 334–343.

[33] Nie, X. W., Y. Du, and H. H. Xu. First-principles studies on structural and electronic properties of $TaCr_2$ Laves phase. *Physica B: Condensed Matter*, Vol. 40520, 2010, pp. 4279–4282.

[34] Vanderbilt, D. Soft self-consistent pseudopotentials in a generalized eigenvalue formalism. *Physical Review B*, Vol. 4111, 1990, id. 7892.

[35] Perdew, J. P., K. Burke, and M. Ernzerhof. Generalized gradient approximation made simple. *Physical Review Letters*, Vol. 7718, 1996, id. 3865.

[36] Monkhorst, H. J. and J. D. Pack. Special points for Brillouin-zone integrations. *Physical Review B*, Vol. 1312, 1976, id. 5188.

[37] Fischer, T. H. and J. Almlof. General methods for geometry and wave function optimization. *The Journal of Physical Chemistry*, Vol. 9624, 1992, pp. 9768–9774.

[38] Kumar, K. S., L. Pang, C. T. Liu, J. Horton, and E. A. Kenik. Structural stability of the Laves phase Cr_2Ta in a two-phase Cr-Cr_2Ta alloy. *Acta Materialia*, Vol. 48, No. 4, 2000, pp. 911–923.

[39] Li, G. F., S. Q. Lu, X. J. Dong, and P. Peng. Microcosmic mechanism of carbon influencing on $NiTiNb_9$ alloy. *Journal of alloys and compounds*, Vol. 542, 2012, pp. 170–176.

[40] Wang, J., S. Yip, S. R. Phillpot, and D. Wolf. Crystal instabilities at finite strain. *Physical Review Letters*, Vol. 7125, 1993, id. 4182.

[41] Thoma, D. J., F. Chu, P. Peralta, P. G. Kotula, K. C. Chen, and T. E. Mitchell. Elastic and mechanical properties of $Nb(Cr, V)_2$ C15 Laves phases. *Materials Science and Engineering: A*, Vol. 239, 1997, pp. 251–259.

[42] Pugh, S. F. Relations between the elastic moduli and the plastic properties of polycrystalline pure metals. *The London, Edinburgh, and Dublin Philosophical Magazine and Journal of Science*, Vol. 45367, 1954, pp. 823–843.

[43] Long, Q., X. Nie, S. L. Shang, J. Wang, Y. Du, Z. Jin, et al. C15 $NbCr_2$ Laves phase with mechanical properties beyond Pugh's criterion. *Computational Materials Science*, Vol. 121, 2016, pp. 167–173.

[44] Hong, S., C. L. Fu, and M. H. Yoo. Elastic properties and stacking fault energies of Cr_2Ta. *Intermetallics*, Vol. 7, No. 10, 1999, pp. 1169–1172.